ISSN 2277-2685
IJESR/April-June. 2023/ Vol-13/Issue-2/219-225
Gandepalli Poornima *et. al.,* / International Journal of Engineering & Science Research

Single Image Haze Removal from an Image Enhancement Perspective for Real-Time Vision Systems

D. Pavana Kumari[1], V. Suresh[2], J Sujatha[3], Gandepalli Poornima[4], Pabireddy Dolly Anusha[5], Lagudu Giridhar[6]

[1,2,3]Assistant Professor, Department of Electronics and Communication Engineering Avanthi Institute of Engineering & Technology, Tamaram, Makavarapalem, Narsipatnam, Anakapalli District – 531113, Andhra Pradesh, India

[4,5,6]UG Student, Department of Electronics and Communication Engineering Avanthi Institute of Engineering & Technology, Tamaram, Makavarapalem, Narsipatnam, Anakapalli District – 531113, Andhra Pradesh, India

Abstract

Vision systems operating outdoors are degraded by atmospheric turbidity, so haze removal has come into use as a pre-processing step for surveillance, remote sensing, navigation and target identification. This paper implements a single image haze removal algorithm intended for real-time use. Rather than inverting the physical model that describes how a hazy image forms, which requires estimating the transmission map and atmospheric light and is computationally expensive, the approach exploits computationally cheaper image processing operations: detail enhancement, multiple-exposure image fusion and adaptive tone remapping. Koschmieder's law is first used to deduce that artificially under-exposed versions of a hazy image contain regions of improved visibility, so that fusing several such exposures recovers a clearer result than any one of them. Detail enhancement is applied before artificial under-exposure by gamma correction, which mimics physical exposure adjustment, and a dark channel prior weighting scheme guides the fusion so that areas with clear visibility are the ones blended into the output. An adaptive tone remapping stage then restores brightness to the darkened fused result. The paper also covers the dark channel prior pipeline in detail, including atmospheric light estimation, transmission map estimation and refinement by bilateral, soft matting and guided filters, and evaluates results using entropy and the image quality index.

Index Terms— *Atmospheric light, dark channel prior, dehazing, guided filter, haze removal, image fusion, tone remapping, transmission map, visibility restoration.*

I. INTRODUCTION

Poor visibility in fog, mist and haze is caused by water droplets suspended in the air. These droplets are small, on the order of 1 to 10 μm, and float steadily. Their presence substantially reduces the visibility of a scene, which becomes a problem for computer vision applications including video surveillance, remote sensing, navigation and target identification.

In India, radiation and advection fog are the most common types, occurring mostly over the north of the country in winter. Advection fog occurs in the forward sector and radiation fog mainly in the rear sector of the synoptic-scale weather systems known as western disturbances. Radiation fog usually forms late at night, when the earth radiates long-wave terrestrial radiation, the air close to the ground is cooled by adiabatic expansion, and saturation conditions are reached; it dissipates after sunrise as the day warms.

A. Types of Fog

Several types are distinguished by their formation mechanism. Radiation fog forms by the cooling of the ground overnight. Advection fog occurs when moist air passes over a cooler surface. Ground fog obscures less than a set fraction of the sky and does not extend to the base of any cloud above. Evaporation or steam fog forms when cool air moves over warmer water. Ice fog forms at very low temperatures, and freezing fog deposits rime as it contacts surfaces. Frontal fog forms near a weather front where rain falls into colder air. Hail fog occurs in the vicinity of significant hail accumulations, and upslope fog forms when moist air is forced up a slope.

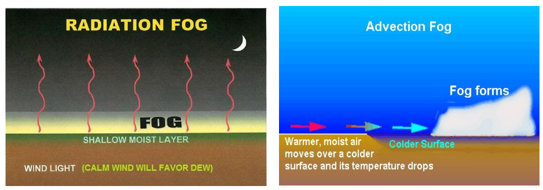

Fig. 1. Radiation fog and advection fog.

B. Atmospheric Optics

The formation of a hazy image is usually described by two effects acting together. Light reflected from the scene is attenuated as it travels to the camera, in proportion to the distance travelled. At the same time, atmospheric light scattered by the particles in the air reaches the camera without having come from the scene at all, and adds to the image as a veil. This second term, the airlight, is what causes distant objects to appear washed towards the colour of the sky, and it grows with distance while the first term shrinks.

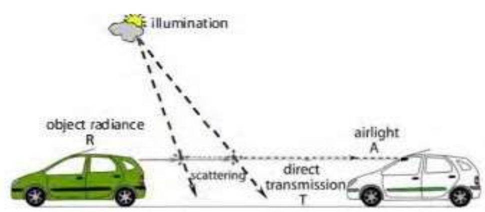

Fig. 2. Airlight and attenuation in a hazy scene.

II. LITERATURE REVIEW

Fattal proposed a method that infers the medium transmission by assuming that the transmission and the surface shading are locally uncorrelated, allowing the two to be separated statistically. The approach recovers a physically plausible result but relies on there being enough variation in the input to estimate the statistics reliably, so it struggles on dense haze where colour information is largely gone.

The dark channel prior, from He et al., observes that in most non-sky patches of an outdoor haze-free image at least one colour channel has very low intensity at some pixels. Where this holds, the intensity actually observed in the dark channel must be due to airlight, which gives a direct estimate of the transmission. The prior is simple and effective and has become the basis for a large family of methods, but its estimation of the transmission map and its refinement are the expensive parts of the pipeline.

Refinement approaches have therefore received considerable attention. Soft matting produces an accurate refined transmission map but solves a large linear system and is slow. The bilateral filter is a widely used edge-preserving smoothing operator and is faster, though its behaviour near strong edges is not ideal. The guided filter has edge-preserving smoothing properties comparable to the bilateral filter with a computational cost independent of the filter radius, which is why it has largely superseded soft matting for transmission refinement.

Xuan Dong et al. developed a fast, efficient algorithm for enhancing low-lighting video, which is relevant because the inverted hazy image resembles a low-light image, and enhancement methods designed for one can be applied to the other. Methods based on enhancement rather than on inverting the physical model form the family that the present work belongs to.

III. DARK CHANNEL PRIOR PIPELINE

DCP-based dehazing is composed of four major steps: atmospheric light estimation, transmission map estimation, transmission map refinement, and image reconstruction.

A. Atmospheric Light Estimation

Most conventional DCP methods estimate the dark channel from the input hazy image, and the only parameter to be determined is the size of the local patch. Its effect is significant, yet most methods either use a fixed size or do not specify it. An image with little local texture and heavy haze needs only a small patch, which reduces the calculation time. An image with complicated local texture needs a larger patch to exclude false texture from the dark channel. But the block-minimum operation inevitably reduces the apparent resolution of the dark channel as the patch grows, so the smallest patch size that does not produce false texture must be found for each image, trading resolution against correctness.

B. Transmission Map Estimation and Refinement

The transmission map describes what fraction of the light from each scene point reaches the camera unattenuated, and it is estimated from the dark channel. The raw estimate is blocky, because it inherits the patch structure of the dark channel computation, so it must be refined against the input image to align its edges with the actual scene boundaries.

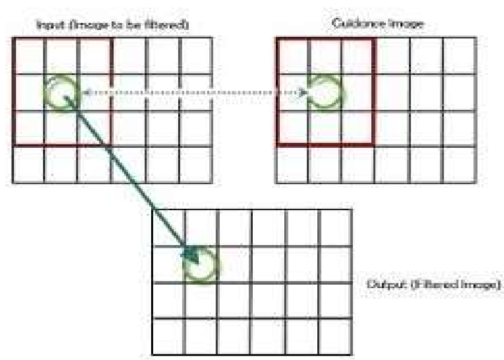

Fig. 3. Guided filter for transmission map refinement.

The guided filter is used for this refinement. Its output within a window is a linear function of the guidance image, with coefficients:

$$a_x = (\mu_x - \bar{\mu}) / (\sigma^2_x + \varepsilon)\ ,\quad b_x = \bar{\mu} - a_x \mu_x \qquad (1)$$

where μ_x and σ^2_x are the mean and variance of the guidance image within the window and ε is a regularization parameter. Because the output is linear in the guidance image, an edge in the guidance image is preserved in the output, which is why the refined transmission map follows the object boundaries in the scene. Since the windows overlap, each pixel's final value is averaged over all windows containing it.

IV. PROPOSED METHOD

The proposed algorithm avoids inverting the physical model. The reasoning starts from Koschmieder's law: because the hazy image is a mixture of attenuated scene radiance and airlight, reducing the exposure of the hazy image reduces the airlight contribution disproportionately in regions where the scene is bright, so an artificially under-exposed version of a hazy image has better visibility in those regions than the original. No single exposure improves the whole image, but different exposures improve different regions, so fusing several of them recovers a result that is clearer throughout. This is what allows the expensive estimation of transmission and atmospheric light to be avoided.

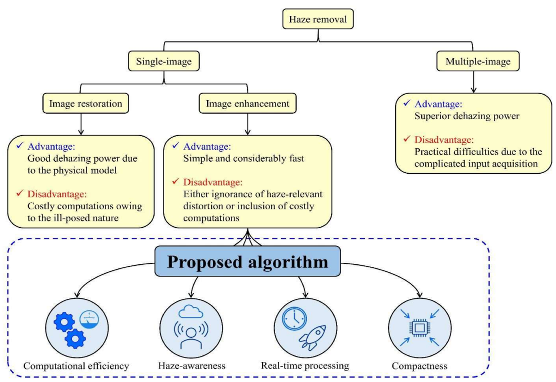

Fig. 4. Block diagram of the proposed algorithm.

A. Detail Enhancement

Detail enhancement is applied before the artificial under-exposure. Gamma correction alone would darken the image uniformly and lose the low-contrast detail that haze has already suppressed; enhancing detail first means that structure survives the subsequent darkening, which is what makes the operation mimic a physical exposure adjustment rather than a simple intensity scaling.

B. Multiple-Exposure Fusion

Several under-exposed versions are generated by gamma correction with different exponents, and these are fused. The weighting scheme is derived from the dark channel: regions whose dark channel indicates low haze, and therefore clear visibility, receive higher weight in the fusion. This is the point at which the dark channel prior enters the method — not to estimate a transmission map to be inverted, but as an indicator of which regions of which exposure are worth keeping, which is a much cheaper use of the same observation.

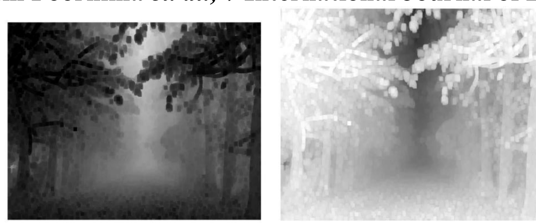

Fig. 5. Input hazy image and pre-processed image.

Fig. 6. Atmospheric light estimation and transmission map estimation.

C. Adaptive Tone Remapping

Fusing under-exposed images necessarily produces a dark result, since every input was darkened. An adaptive tone remapping stage restores brightness, adjusting the mapping according to the content of the fused image rather than applying a fixed curve, so that the recovered detail is presented at a usable brightness without the bright regions being clipped.

V. QUALITY PARAMETERS

A. Entropy

Image entropy describes the amount of information in an image. Low-entropy images, such as those containing large areas of uniform sky, have little contrast and long runs of similar pixel values, and can be compressed to a small size; a perfectly flat image has entropy zero. High-entropy images have substantial variation between adjacent pixels and compress less. Entropy is computed as:

$$Entropy = -\sum_i P_i \log_2 P_i \quad (2)$$

where P_i is the probability that the difference between two adjacent pixels equals i. For dehazing, entropy is a useful measure because haze suppresses local contrast, so a successful removal should raise the entropy of the image relative to its hazy input.

B. Image Quality Index

For an original image f(x, y) and a defogged image g(x, y) of dimension M × M, the image quality index combines three factors: the correlation between the two images, the closeness of their mean values, and the similarity of their variances. It is computed as:

$$IQI = 4\,\sigma_{fg} \cdot \bar{f} \cdot \bar{g} \,/\, [\,(\sigma^2_f + \sigma^2_g)(\bar{f}^2 + \bar{g}^2)\,] \quad (3)$$

where $\bar{f}$ and $\bar{g}$ are the means and σ^2_f and σ^2_g the variances of the two images, and σ_{fg} their covariance.

VI. RESULTS AND DISCUSSION

The algorithm was evaluated on hazy images, comparing the defogged result without pre-processing, with pre-processing, and after fusion.

Fig. 7. Defogged output without pre-processing and with pre-processing.

Fig. 8. Defogged results for further test images.

Fig. 9. Comparison of results before and after fusion.

Applying detail enhancement before under-exposure produced visibly better results than under-exposure alone, confirming the reasoning behind the ordering of the two operations: the detail that gamma correction would otherwise suppress is what carries the scene structure in hazy regions. The fusion stage combined the exposures without the halo artefacts that appear when a transmission map is inverted with an inaccurate estimate, which is a consequence of never forming that estimate.

Entropy rose for the defogged images relative to their hazy inputs, consistent with the recovery of local contrast that haze had suppressed. The computational advantage of the approach comes from what it omits: no transmission map is estimated and refined, and no atmospheric light is solved for, so the operations that remain are gamma correction, filtering and weighted summation, all of which are local and inexpensive.

VII. CONCLUSION AND FUTURE SCOPE

A computationally efficient haze removal algorithm was implemented. Dehazing methods based on the Koschmieder model are computationally expensive, mainly because of the unavoidable estimation of unknown variables, namely the transmission map and the atmospheric light. Koschmieder's law was instead used to deduce the value of under-exposed images for haze removal, and simple image processing operations — detail enhancement, gamma correction, single-scale image fusion and adaptive tone remapping — were used to realize that deduction.

Detail enhancement before artificial under-exposure by gamma correction effectively mimics physical exposure adjustment, while the dark channel-based weighting scheme guides the fusion so that areas of clear visibility are the ones blended into the result. The adaptive tone remapping stage then restores the brightness lost in fusing darkened inputs.

Because the pipeline consists only of local operations with no global solve, it is suited to hardware implementation, and this is the direction in which the work would continue: a compact design capable of sustaining video frame rates would allow the method to be integrated as a pre-processing stage in an existing real-time vision system, which is where haze removal is most useful.

References

[1] K. He, J. Sun, and X. Tang, “Single image haze removal using dark channel prior,” IEEE Transactions on Pattern Analysis and Machine Intelligence, vol. 33, no. 12, pp. 2341–2353, 2011.

[2] K. He, J. Sun, and X. Tang, “Guided image filtering,” IEEE Transactions on Pattern Analysis and Machine Intelligence, vol. 35, no. 6, pp. 1397–1409, 2013.

[3] R. Fattal, “Single image dehazing,” ACM Transactions on Graphics, vol. 27, no. 3, pp. 1–9, 2008.

[4] R. T. Tan, “Visibility in bad weather from a single image,” in Proc. IEEE Conf. Computer Vision and Pattern Recognition (CVPR), 2008, pp. 1–8.

[5] S. G. Narasimhan and S. K. Nayar, “Contrast restoration of weather degraded images,” IEEE Transactions on Pattern Analysis and Machine Intelligence, vol. 25, no. 6, pp. 713–724, 2003.

[6] X. Dong, Y. Pang, and J. Wen, “Fast efficient algorithm for enhancement of low lighting video,” in ACM SIGGRAPH 2010 Posters, 2010.

[7] C. Tomasi and R. Manduchi, “Bilateral filtering for gray and color images,” in Proc. IEEE Int. Conf. Computer Vision (ICCV), 1998, pp. 839–846.

[8] A. Levin, D. Lischinski, and Y. Weiss, “A closed-form solution to natural image matting,” IEEE Transactions on Pattern Analysis and Machine Intelligence, vol. 30, no. 2, pp. 228–242, 2008.

[9] Q. Zhu, J. Mai, and L. Shao, “A fast single image haze removal algorithm using color attenuation prior,” IEEE Transactions on Image Processing, vol. 24, no. 11, pp. 3522–3533, 2015.

[10] D. Berman, T. Treibitz, and S. Avidan, “Non-local image dehazing,” in Proc. IEEE Conf. Computer Vision and Pattern Recognition (CVPR), 2016, pp. 1674–1682.

[11] T. Mertens, J. Kautz, and F. Van Reeth, “Exposure fusion,” in Proc. Pacific Conf. Computer Graphics and Applications, 2007, pp. 382–390.

[12] Z. Wang and A. C. Bovik, “A universal image quality index,” IEEE Signal Processing Letters, vol. 9, no. 3, pp. 81–84, 2002.

[13] W. E. K. Middleton, Vision Through the Atmosphere. University of Toronto Press, 1952.

[14] R. C. Gonzalez and R. E. Woods, Digital Image Processing, 4th ed. Pearson, 2018.